Chapter 3

Out of Autoclave Metal and FRP Composites Thermo-Hydroforming

Bo C. Jin, Xiaochen Li, Karl Neidert and Michael Ellis

Additional information is available at the end of the chapter

http://dx.doi.org/10.5772/intechopen.81600

Abstract

In this chapter, we explore a novel type of thermo-hydroforming process conceived to expand the role of sheet metal hydroforming machines from one of just forming sheet metal materials into one of being able to form multiple materials. This work specifically focuses on the use of thermohydroforming to shape and thermal catalyze prepreg composite sheets into rigid parts of complex 3D geometry. Elastomeric Sheet Hydroforming is an excellent low-cost manufacturing method requiring a single tool die on only one side. The mating die is a flexible membrane backed by fluid under high pressure. Various designs configurations exist that allow for significant pressure levels of up to 1400 Bar (20,000 psi), to be contained. The cycle life of the containment vessel components is commonly designed to accommodate up to 1 million cycles of use over 40 years. However, these machines can be expensive ranging in cost from several hundred thousand up to $6 million dollars. Expanding the market scope and potential of the press by enabling them to also form composites will provide benefit to both the machine owners and their customers. The intent of this project is to advance the state of the art in composites forming by demonstrating through FEA modeling that a hydroforming machine can be potentially configured to form thermally catalyzed prepreg composite panels. It is believed that the concept in like manner, will also be applicable to forming metal-composite hybrid panels, stratified metal thermoplastic laminates, thermoplastic synthetic granites and of course sheet metal materials. This concept seeks to benefit the American Manufacturing Industry and create jobs in the U.S. by providing a low-cost method for manufacturers to produce medium to very large sized high-quality sheet composite parts of an advanced nature in construction. This application is for operations requiring volumes less than 30,000 forming cycles per year per machine. Processes currently exist in the industry that utilizes heated air or heated glycol to form sheet materials. However, this process seeks to offer greater benefit by using pure water as a high thermal conductivity working fluid in a scheme that offers vastly elevated pressure during forming and curing cycles.

Keywords: thermo-hydroforming, novel manufacturing methods for composite materials

1. Introduction

1.1. Background: identification and significance of the innovation

1.1.1. General information

Sheet hydroforming is a process that was primarily developed for the needs of the aircraft industry. In sheet hydroforming, formed tooling blocks are placed in the machine's loading tray and pre-cut sheet metal blanks are placed over the blocks. Throw pads are then placed over the blanks to cushion sharp edges. The tray is then fed into the pressing chamber as a thick elastic blanket is unrolled over the tool and sheet metal. The pressure chamber is a thick-walled cylinder wound with high tensile strength metal wire that is engineered to handle the extremely high forming pressures. Once the part is loaded, immensely high fluid backfill pressure is applied to the membrane. The elastic blanket diaphragm expands and flows downward, over and around the metal blank. The sheet metal is then pressed to follow the contour of the die block, exerting an even, positive pressure at all contact points. As a result, the metal blank is literally wrapped to the exact shape of the die block. The press is then depressurized for unloading the tray. This process is ideal for prototyping and low volume production in aluminum, titanium, stainless steel, and other aerospace alloys such as matrix metal panels in low volumes [1, 2].

1.2. Customer problem

1.2.1. Automotive

The new fuel economy standards which mandate an average fuel economy of 54.5 miles per gallon for the 2025 model year will highly motivate auto manufacturers to step up development of improved vehicle designs and technologies to sharply improve the fleet mileage. Mass produced models will need to utilize more efficient engines and new lighter but safe car bodies. Automobile manufacturers have investigated alternatives to the steel traditionally used in car production. However, in most cases, the on-road properties of steel make it the best choice for automotive fabrication [3]. As a result, we are seeing a renewed interest in the use of high-strength steel and composites.

Carbon-fiber composite car structures are now in vogue. BMW produces two all carbon electric vehicle designs the i3 and the i8. General Motors' Corvette Stingray has a carbon-fiber roof and hood. Other recent autos that feature carbon-fiber-reinforced polymer (CFRP) components include the Audi R8, the BMW M6, and the Dodge Viper. Most of these models, however, are high end, low-volume vehicles that are mainly assembled manually because composites use in low and medium-priced cars is still awaiting the development of cost effective mass-production processes and materials [4, 5].

1.2.2. Aerospace: NASA general aviation program

The goal of the NASA General Aviation Program is to reduce public travel times by half in 10 years and by two-thirds in 25 years. To accomplish this goal, NASA and its partners are pursuing development of the revolutionary technologies necessary not only to build the next generation of vehicles for business and personal air transportation but also to train the average person to operate them safely. Low cost composite panels are vital to the success of NASA's program which supports electric aircraft and H.R. 1848, "The Small Airplane Revitalization Act" [6–8].

1.3. Modern architecture

The world has recently seen massive advancements in architecture. Numerous buildings in places such as Dubai have advanced the state of the art well beyond previous construction methods. Leading architects such as Frank Gehry, Zaha Hadid, and others are deep in a renaissance of building construction esthetics and methodologies.

Structures fabricated from numerous unique panels are especially well suited to production applications. Computer Aided Design (CAD) software is now used to convert complex 3D geometric forms into numerous 3D architectural SIP (Structural Insulated Panels) panels of a manageable size and shape. The panelized surface architecture process can be applied to buildings, sculptures, ships and aircraft [9].

2. Out-of-autoclave (OOA) composites hydroforming approaches

2.1. Out of autoclave sheet composites forming methods

2.1.1. Globe machine manufacturing

The Globe Company (**Figure 1**) now produces a pressurized air driven bladder technology that is used to form body panels for the Chevy Corvette. This process uses 300 psi of air with a 0.5 mm silicone sheet bladder to pressure bag form parts. They are currently supporting volumes of 34,000 vehicles a year [10, 11].

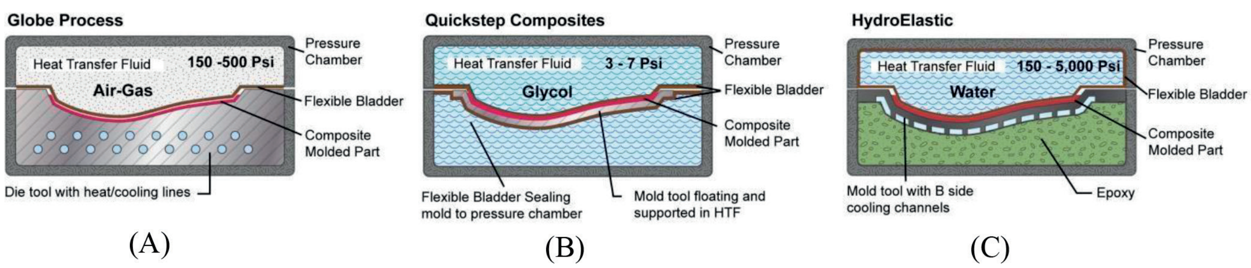

Figure 1. Cross sections of processes: (A) globe manufacturing (left); (B) quickstep composites (middle); (C) hydrothermal hydroforming (right).

2.1.2. Quickstep composites

Quickstep is an Australian-listed company. The Quickstep process forms composite parts using 4 psi (low pressure) on a rigid tool suspended between two elastomeric membranes back filled with glycol fluid. Their large format out of autoclave forming and curing process works well for large parts. Aerospace parts such as wing skins can be molded using either prepreg materials or resin injection molding [12, 13].

2.1.3. Thermo-hydroforming

In this chapter, an "Out of Autoclave (OOA) HydroElastic Hydroforming" method is proposed to utilize pressurized water as a forming fluid behind an elastomeric membrane. The shell tool is water heated and backed by a high strength reusable fiber/epoxy composite [14–24]. In addition to the forming chamber shown, an outer sleeve chamber is used to contain extremely high pressures [25, 26]. Because of this high-pressure capability, the system can simultaneously form laminate stacks of both metal and composite material strata using the OOA hydroforming approach. This opens new potential possibilities for metal [27–32] and fiber reinforced composite flat panel [33–35] as well as contoured part designs [36, 37].

2.2. GLARE® laminate with S-2 glass fiber by AGY

One of the most exciting materials under evaluation for primary and secondary aircraft components is GLARE laminate. Glass Laminate Aluminum Reinforced Epoxy (GLARE) is a sandwich material constructed from alternating layers of aluminum and S-2 Glass® fiber with bond film. The material, developed at Delft University of Technology in the Netherlands, has been recognized as one of the top aerospace materials for the future.

It is believed that thermo-hydroforming has the potential to form GLARE multi-sheet material stacks. This would create a 3D conformal forming process that allows full design engineering of complex 3D shaped parts as needed. The parts are formed in a tool die that allows the part to be configured exactly as needed for the specified function. In addition, thermo-hydroforming forming, will enable subtle surface inflections to be made in parts for things such as flush access doors, flush rivets and flanges as well as embedded cast–forged, electrical or intelligent components.

2.3. Technical objective

This project seeks to gain a foundational understanding of the proposed thermo-hydroforming machine's performance by conducting FEA simulations [38–40]. This simulation studies a multiply coupon of carbon fiber prepreg being formed by a vulcanized silicone elastomeric bladder. The bladder is heated and pressed into the composite coupon by water heated to 285°F under 300 psi of pressure. The tool is pre heated to the temperature of 285°F as well. As a result, the composite coupon is heated from above and below. This process should be used comfortably to 425°F (218°C) and 10,000 psi/700 Bar.

We understand from work by Globe manufacturing, Quickstep Composites and other prior art that both air and fluid heat behind a membrane can be used to react and cure prepreg materials. It is also known that pure water has one of the best thermal conductors. Water has a thermal conductivity that is 24 times greater than that of air and that circulating water increases this effectiveness even further by a factor of 10. Our objective is to study the viability of adopting these methodologies to hydroforming.

Hydroforming has a well-documented history of safely forming sheet metal materials at pressures of up to 20,000 psi (137.89 Mpa) well beyond the requirements of composite materials. Because hydroforming machines can deliver and contain high fluid pressure, it is believed that the addition of a thermal cycle to heat & cool the forming chamber's working fluid will enable a significant industrial advancement in sheet hydroforming machines. The new methodology will allow for a single machine to shape, catalyze and cure prepreg composite materials, thermal plastics and matrix materials in addition to its traditional use as a metal forming machine.

With FEA simulations demonstrated, qualitative assessments can be made to facilitate the future validity for development, implementation and commercialization of thermo-hydroforming machinery.

3. Fluid properties for thermal-hydroforming

Fresh water has a very high level of thermal conductance. It is 100% better than glycerol and 350% better than machine oil. However, in order to be used at high temperature water must be pressurized to prevent boiling. In this design configuration pressure is applied as a part of the process. As a result, at 300 psi water can be used at temperatures of approximately 400°F (**Figures 2** and **3**).

4. FEA simulation: thermal-hydroforming of composites

4.1. Analysis type and geometry

The first load step consists of a linear static analysis where only the pressure load is applied. This allows for the composites to be in contact with the tool. Following this, a transient coupled thermal displacement step is run to obtain the temperature distribution and heat flux through time. Total time used was 200 s.

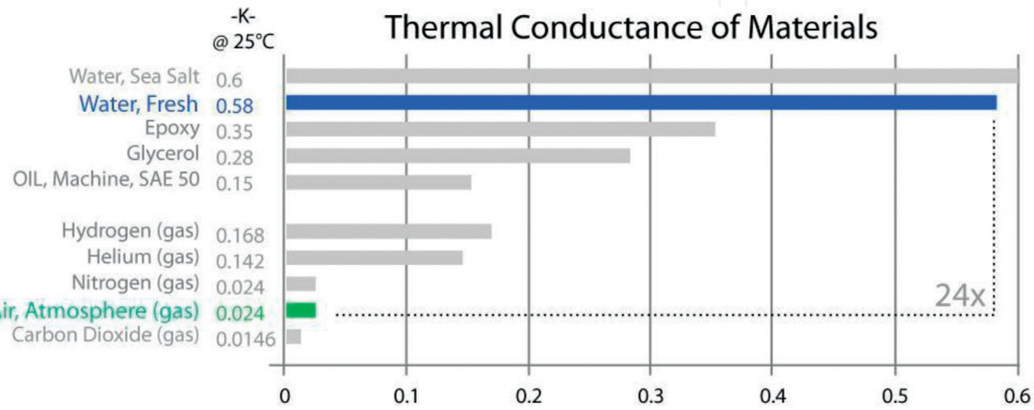

Figure 2. Thermal expansion of select materials.

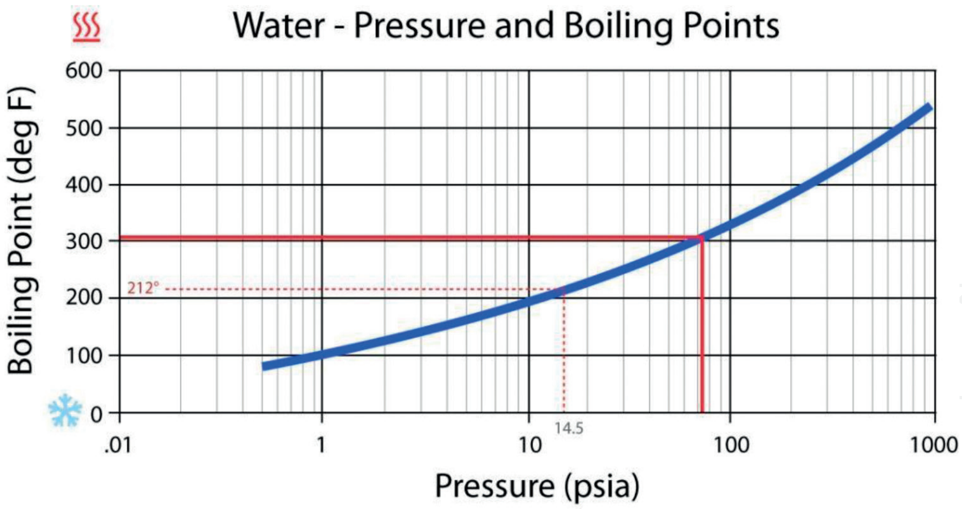

Figure 3. H_2O pressure vs. boiling temperature.

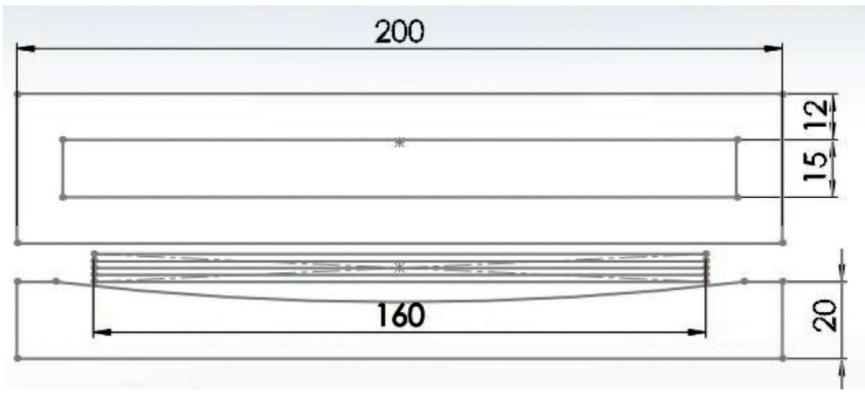

Figure 4. General dimensions of the model.

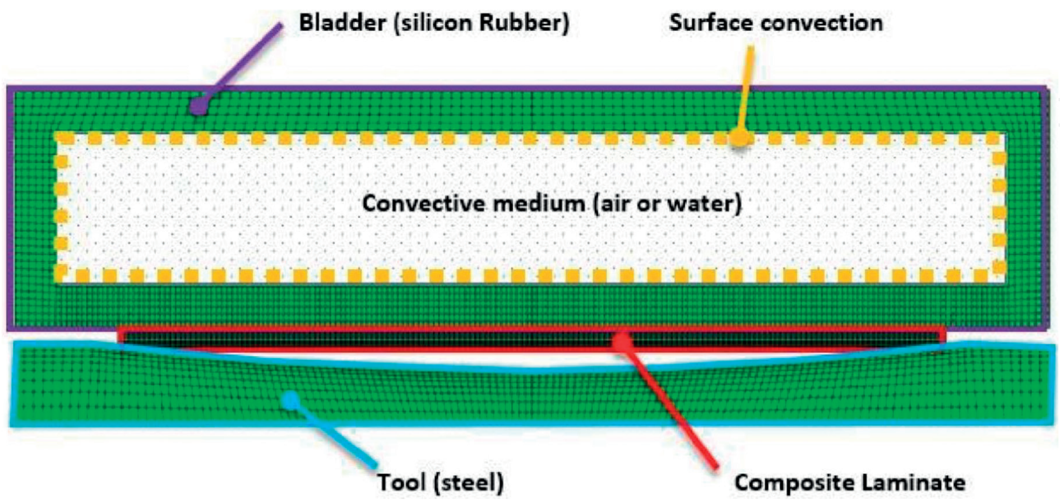

Figure 5. Assigned materials for each component.

http://dx.doi.org/10.5772/intechopen.81600

The geometry consists of an expandable silicon rubber bladder, which contains a convective medium inside. This convective medium is not modeled, however, the effects of convection on the general temperature distribution are important and therefore, simulated. Two different bladder thicknesses were evaluated: 6 mm and 12 mm. The bladder sits on top of a Torayca 300 carbon/epoxy prepreg laminate consisting of the following stacking order: $(0, -45, 90, 45)_2$. The laminate sits on top of a concave aluminum tool (**Figures 4** and **5**).

4.2. Load steps

a) The rubber bladder at room temperature is pressurized with hot fluid (285°F). The bladder heats up by convection until it reaches thermal equilibrium with the hot fluid.

b) The Rubber bladder expands downward due to the exerted pressure of 300 psi and pushes the composite laminate onto the aluminum tool which is also heated to 285°F.

c) The composite laminate which has a cold OTF (Out of Freezer) temperature of 65°F is heated by the tool and rubber bladder by means of thermal conduction until thermal equilibrium is achieved.

4.3. Thermomechanical properties input

The following mechanical and thermal properties (**Tables 1–3**) of the respective component's material were assigned to the different parts to proceed with the FEA simulations.

4.4. Boundary conditions

Shown in **Figure 6**, the bladder is fixed from the top, to allow the bottom to expand downward, pushing the composites towards the tool. The tool is also fixed so the compressive load is applied to the composites.

4.5. Loading conditions

Shown in **Figure 7**, a uniform pressure of 300 psi was applied to the bottom inner surface, to simulate the bladder expansion which pushes the composite towards the tool. Initial temperatures assigned to the parts were shown in figure.

Material	Elastic modulus (Mpa)	Poisson ratio	Density (Ton/mm^3)
Composite Laminate	135,000	0.3	1.76E-09
Steel	210,000	0.3	7.89E-09
Silicon Rubber	50	0.48	1.70E-09

Table 1. Mechanical properties of assigned materials.

Material	Heat conductivity specific heat	
	Coefficient (mJ/mm K)	(mJ/Ton K)
Composite Laminate	10.46, 7.2, 9	795,000,000
Steel	43	466,000,000
Silicon Rubber	1.375	1,180,000,000

Table 2. Thermal properties of assigned materials.

Material	Convection coefficient (mW/mm² K)	Efficiency
Free air	0.0015	1X
Free water	0.06	40X
Moving water	5.15	3433X

Table 3. Convection coefficients for different liquids.

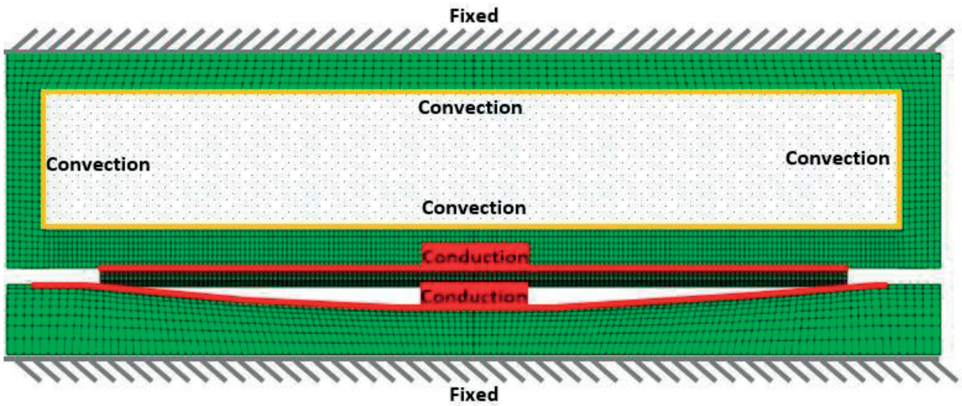

Figure 6. Boundary conditions applied to the model.

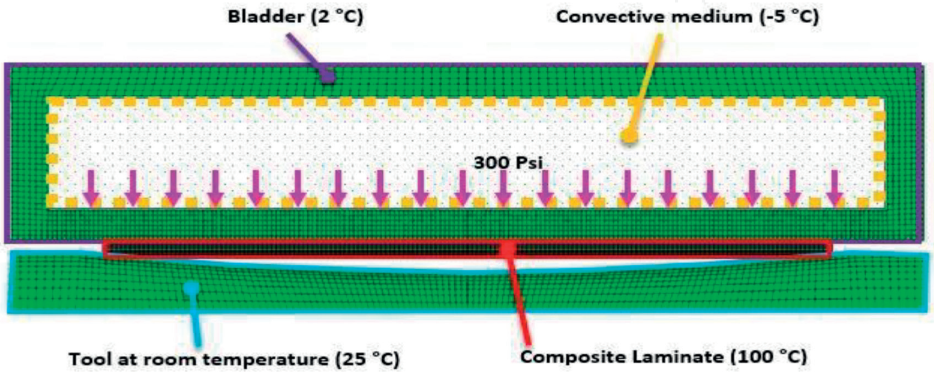

Figure 7. Initial temperatures for each part.

http://dx.doi.org/10.5772/intechopen.81600

4.6. FEA results

4.6.1. Load step 1: bladder heating

During this first load step, thermal conduction between the bladder and the composite laminate is ignored, this allows for the display of the thermal contour of the bladder as it heats up due to convection (**Figures 8–11**).

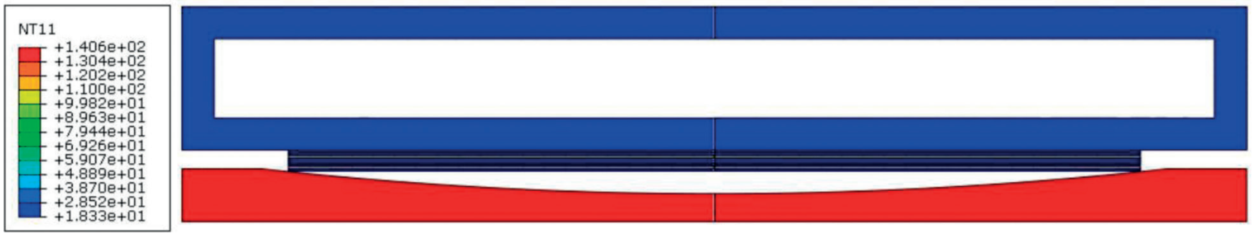

Figure 8. Nodal temperature results at t = 0 s (initial state).

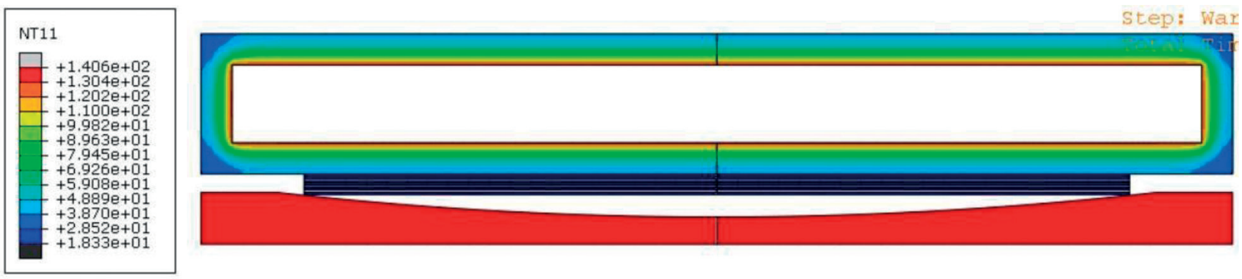

Figure 9. Nodal temperature results at t = 8.38 s.

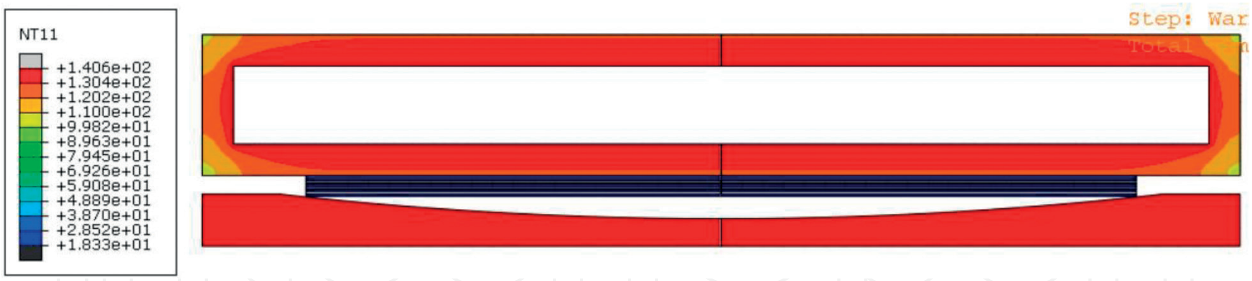

Figure 10. Nodal temperature results at t = 70 s.

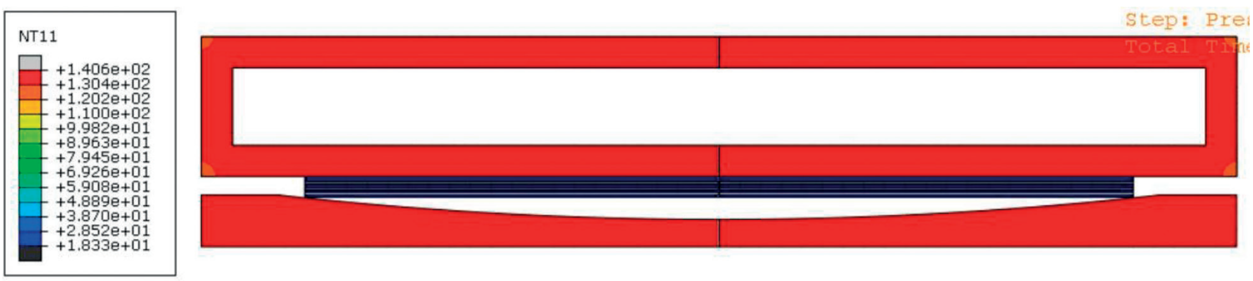

Figure 11. Nodal temperature results at t = 120 s (bladder completely heated up).

4.6.2. Load step 2: bladder expansion

Once the bladder is at operating temperature (285°F), the expansion due to the fluid's pressure is simulated. This makes the bladder expand, which consequently pushes the composite plate towards the concave aluminum tool (**Figure 12**).

4.6.3. Load step 3: curing by thermal conduction

The final load step in the simulation is to enable the thermal conduction between the bladder and the tool towards the cooler composite laminate (**Figures 13–18**).

Additionally, one element per composite layer was probed to analyze its temperature through time. The selected elements were those in the symmetric center of the composite laminate. The same procedure was used for the bladder, to measure the time required for it to reach its working temperature (**Figures 19–23**).

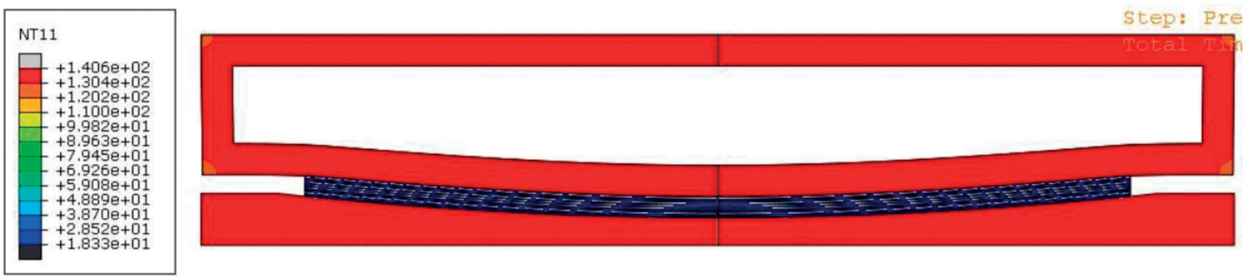

Figure 12. Expanded bladder due to applied pressure of 300 psi (the composite plate and tool are in contact).

Figure 13. Nodal temperature results at t = 120 s (respective to current load step).

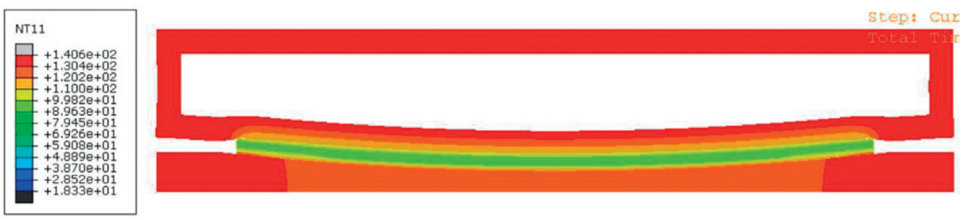

Figure 14. Nodal temperature results at t = 130 s, t = 120 s (respective to current load step).

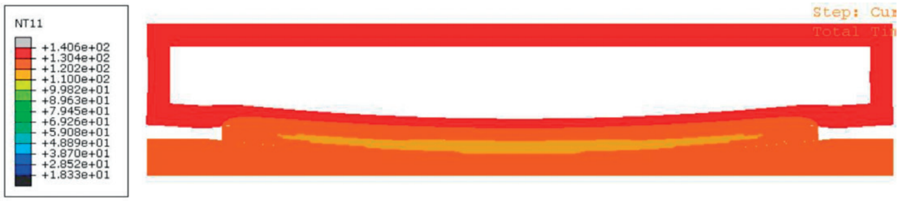

Figure 15. Nodal temperature results at t = 147 s (respective to current load step).

Figure 16. Nodal temperature results at t = 274 s (respective to current load step).

Figure 17. Nodal temperature results at t = 338 s (respective to current load step).

Figure 18. Nodal temperature results at t = 438 s (respective to current load step).

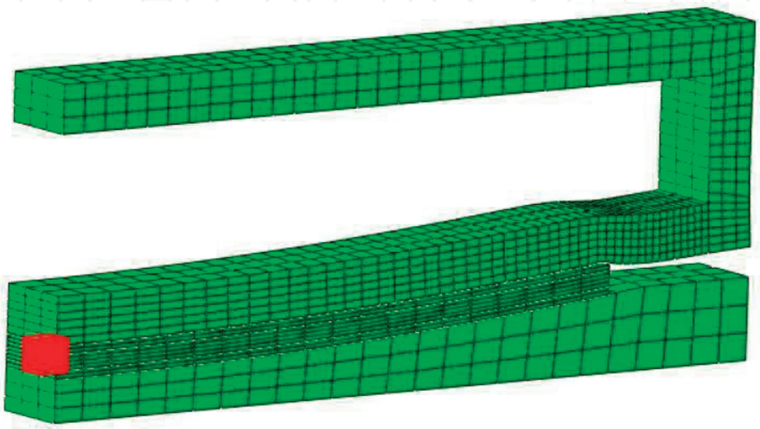

Figure 19. Nodes selected for plotting the temperature gradient throughout the composite material thickness.

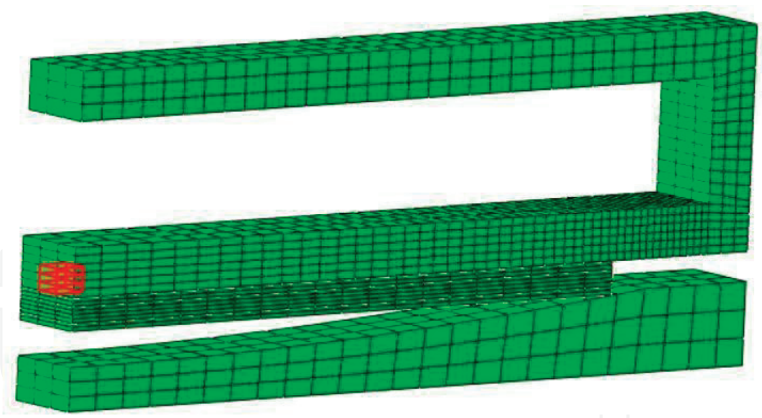

Figure 20. Nodes selected for plotting the temperature gradient throughout the composite material thickness.

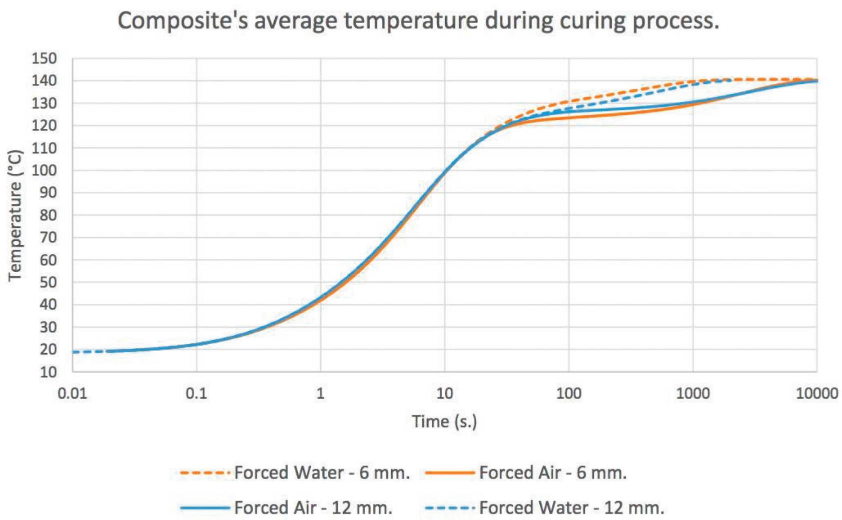

Figure 21. Composite temperature history.

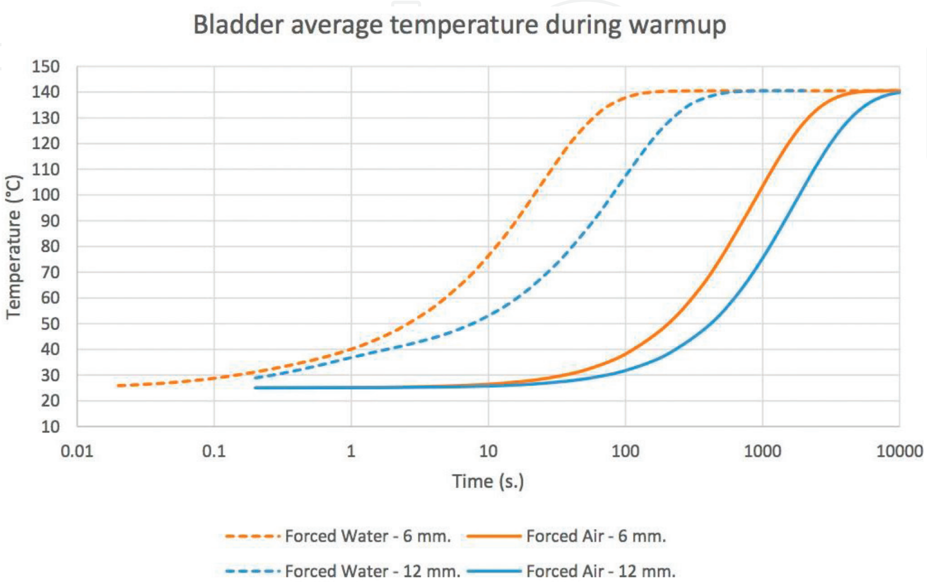

Figure 22. Bladder temperature history.

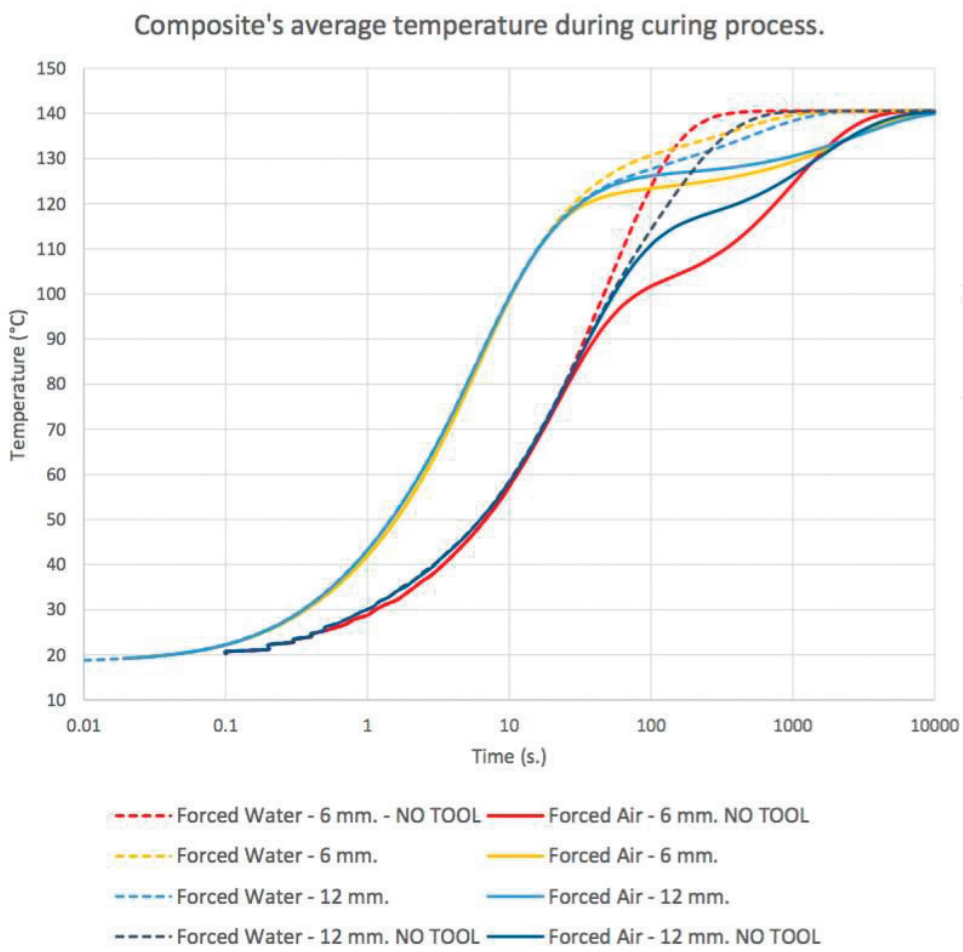

Figure 23. Effect of the aluminum tool on the overall curing process.

5. Conclusions

It can be concluded that both air and water provide similar curing temperatures for the composite laminate, however, the warm-up time is considerably different for the two convective mediums as it can be observed in the above presented results. Air is considerably slower in warming up the silicon bladder up to operating temperature. Once the aluminum tool and the silicon bladder are at operating temperature, the bladder thickness nor the convective medium have much effect on the overall curing process time. It is only until the very end that the different convective mediums display different curing rates.

Based on results of the simulation provided, the use of a snap cure epoxy binder, and an additional 90 second cycle to cool the part; It seems highly probable that parts can be formed in a hydroforming machine in approximately 10 min. With the addition of residual heat in the bladder and some process optimization it may be possible to reduce the actual cycle time 30% further to 7 min. Physical experiments are needed for validation.

A large hydroforming tray bed may be able to form 4–6 parts in one cycle. A 10-min cycle running 4 parts produces a 2.5-min average part cycle time. A 250 days' work year, running a 7-h shift would produce 42,000 parts per year. The envisioned ability to form and cure metal composite laminated parts in one single hydroforming process step has yet to be physically proven, but based on simulations it is highly promising. More in-depth study and physical models will be required to fully validate the process. However, based on the initial work completed, it seems viable to project, that a hydroforming machine can be used to form composite parts.

It also seems viable that a hydroforming machine is well suited to accommodate the high pressures required by some snap-cure resins such as HexPly M77. This particular resin requires a pressure of 80 bar (1160 psi). Over a large wide surface area, 80 bar will generate significant force. However, hydroforming machine are designed for much greater loads and would easily accommodate the level of pressure. The ability to co-form metal alloys and composite materials seems to be viable and is believed to be a topic worthy of additional study.

Vehicles produced for H.R. 4013 (IH)—Low Volume Motor Vehicle Manufacturers Act of 2014, 2025 CAFÉ Corporate Average Fuel Economy mpg target of 54.5 and the needs of General Aviation, advancement especially electric aircraft may attain benefits from this study.

6. Potential future opportunities

6.1. Unique industry applications and possible advancements resulting from concept development

- Typology Optimized Structural Sandwich Panels (SSP)
- SSP Panels and skin panels with embedded electrical circuits, sensors, induction fields
- SHM Structural Health Monitoring of panels
- Heating from above and below accommodates use of panel cores with insulating properties such as porous media, foams gels and ceramics
- 3D structural battery or structural capacitor skin panels
- Power and communications integral to panels
- Induction field-based panel warping
- Induction field based electromagnetic lock downs and energy pick up
- Large area pressure sensitive/pressure monitoring panels or tiles
- Embedded surface heating for de-icing
- Damaged Part and Part Deflection Detection/SHM Structural Health Monitoring
- Insertion of “Heavy Inserts” such as ceramics, castings, forgings or computers
- Large 3D conformal structural storage tanks for liquid or air-gas fuel
- Electric vehicles, electric aircraft, robotics
- Integration of EAP (Electroactive Polymer) into skin panels

6.2. Electroactive polymer (EAP)

Electroactive Polymer (EAP) is a polymer that exhibits a change in size or shape when stimulated by an electric field. The field generates coulomb attractive forces on the electrodes that apply compressive forces on the dielectric causing the change in size or shape. There are three primary types of EAP: Ionic, Piezoelectric and Dielectric. EAP can be used to create a variety of devices including sensors, actuators, and energy harvesting devices. Inclusion of EAP into composites laminate sandwich panels may have potential for a few excellent features such as vibratory deicing or wing warping.

Author details

Bo C. Jin[1]*, Xiaochen Li[1], Karl Neidert[2] and Michael Ellis[3]

*Address all correspondence to: bochengj@usc.edu

1 Research Scientist, Aerospace and Mechanical Engineering, University of Southern California, California, United States

2 Patent Attorney, Karl Neidert and Associates, CA, United States

3 CTO, Ellis Industrial Design, San Diego, CA, United States

References

[1] Enprotech Hydroforming. http://www.enpromech.com/hydroforming-fluid-cell/

[2] Triform Hydroforming http://www.triformpress.com/?gclid=COel8ZXM7cYCFY17fgodXEIKhQ

[3] Grelling Keane. http://www.bloomberg.com/news/articles/2011-0729/automakers-agree-to-54-5-mpg-u-s-fuel-economy-rule-obama-says

[4] Composites World. http://www.compositesworld.com/blog/post/in-new-corvette-stingrayanother-step-forward-for-composites

[5] Plasan Carbon Composites Corvette Marketing Materials http://plasancarbon.com

[6] Conner, Monroe. http://www.nasa.gov/centers/armstrong/Features/leaptech.html

[7] Kim HD, Brown GV and Felder JL. NASA Glenn Research Center Cleveland Ohio: Distributed Turboelectric Propulsion for Hybrid Wing Body Aircraft; 2008 July 24

[8] Rep. Pompeo, Mike. https://www.congress.gov/bill/113th-congress/house-bill/1848; 2013, May 7

[9] Eigensatz M, Kilian M, Schiftner A, Mitra NJ, Pottmann H, Pauly M, Evolute Software. 2010. http://www.evolute.at/software-en/evolutetools-for-rhino, http://vecg.cs.ucl.ac.uk/Projects/SmartGeometry/paneling/paper_docs/panelization_sigg10_small.pdf

[10] US 20140134382 A1, Ronald M. JACOBSEN. Thermal Processing and Consolidation System and Method, Globe Machine Manufacturing Company; May 15, 2014

[11] US8650745 B2 Ronald M. JACOBSEN. Thermal Processing and Consolidation System and Method, Globe Machine Manufacturing Company; Feb 18, 2014

[12] US 7497981 B2 Neil Graham. Composite and Metal Component Production, Forming and Bonding System; Mar 3, 2009

[13] US8580176 - Q/S Neil Graham. Systeme de liaison, de formation et de production de composite et de composant metallique; Aug 1, 2002

[14] Jin B, Pelegri A. Three-dimensional numerical simulation of random fiber composites with high aspect ratio and high volume fraction. Journal of Engineering Materials and Technology. 2011;**133**:41014

[15] Jin B, Li X, Jain A, Carlos G, LLorca J, Nutt S. Optimization of microstructure and mechanical properties of composite oriented strand board from reused prepreg. Journal of Composite Structures. 2017;**174**:389-398

[16] Wu M, Jin B, Nutt S. Processing and performance of recyclable composites for wind turbine blades. Advanced Manufacturing: Polymer & Composites Science. 2019;**12**:12-28

[17] Jin B, Li X, Jain A, Wu M, Mier R, Herraez M, et al. Mechanical properties and finite element analysis of reused UD carbon fiber/epoxy OoA VBO composite oriented strand board. In: Proceedings of SAMPE 2016; Long Beach. 2016

[18] Jin B, Li X, Wu M, Jain A, Jormescu A, Gonzalez C, et al. Nondestructive testing and evaluation of conventional and reused carbon fiber epoxy composites using ultrasonic and stitched micro-CT. In: Proceedings of SAMPE 2016; Long Beach. 2016

[19] Jin B, Li X, Jain A, Wu M, Mier R, Herraez M, et al. Prediction of stiffness of reused carbon fiber/epoxy composite oriented strand board using finite element methodsRecycling Materials & Structures. Feature Article. Society for the Advancement of Material and Process Engineering (SAMPE) Journal. 2017;**53**:32-39

[20] Jin B, Li X, Jain A, Herraez M, Gonzalez C, LLorca J, et al. Development of a finite element model for reused carbon fiber epoxy composite oriented strand board. In: Proceedings of SAMPE 2016; Long Beach. 2016

[21] Jain A, Jin B, Nutt S. Mean field homogenization methods for strand composites. Journal of Composites Part B. 2017;**124**:31-39

[22] Jain A, Jin B, Li X, Nutt S. Stiffness predictions of random chip composites by combining finite element calculations with inclusion based models. In: Proceedings of SAMPE 2016; Long Beach. 2016

[23] Jain A, Jin B, Nutt S. Development of chip composites with improved mechanical performance attributes using hybrid multi-scale modelling methods. In: Proceedings of CAMX 2016; Anaheim. 2016

[24] Jin B. Recent development of reused carbon Fiber reinforced composite oriented Strand boards. In: Chapter of Book: Recent Developments in the Field of Carbon Fibers. Rijeka: Intech Open. DOI: 10.5772/intechopen.71346

[25] Jin B, Mier R, Li X, Neidert K, Nutt S, Ellis M. Design and FEA of a wound composite hydroforming machine under high pressure. In: Proceedings of SAMPE 2015; Baltimore. 2015

[26] Jin B. Sustainable and efficient hydroforming of aerospace composite structures. In: Chapter of Book: Green Sustainable Composites. IntechOpen. In Print

[27] Wu H, Fan G, Jin B, Geng L, Cui X, Huang M. Fabrication and mechanical properties of TiBw/Ti-Ti (Al) laminated composites. Journal of Materials and Design. 2016;**89**:697-702

[28] Wu H, Fan G, Jin B, Geng L, Cui X, Huang M, et al. Enhanced fracture toughness of TiBw/Ti3Al composites with a layered reinforcement distribution. Journal of Materials Science and Engineering: A. 2016;**670**:233-239

[29] Wu H, Jin B, Geng L, Fan G, Cui X, Huang M, et al. Ductile-phase toughening in TiBw/Ti-Ti3Al metallic-intermetallic laminate composites. Journal of Metallurgical and Materials Transactions A. 2015;**46**:3803-3807

[30] Chen Z, Huang T, Jin B, Hu J, Lu H, Nutt S. High yield synthesis of single-layer graphene microsheets with dimensional control. Journal of Carbon. 2014;**68**:167-174

[31] Huang T, Li T, Xin Y, Jin B, Chen Z, Su C, et al. Preparation and utility of a self-lubricating and anti-wear graphene oxide nano-polytetrafluoroethylene hybrid. Journal of RSC Advances. 2014;**4**:19814

[32] Huang T, Jin B, Li X, Li T, Nutt S. Experimental and finite element analysis study of load carrying capacity of modified polyimide. In: Proceedings of SAMPE 2013; Wichita. 2013

[33] Jin L, Jin B, Kar N, Nutt S, Sun B, Gu B. Tension-tension fatigue behavior of layer-to-layer 3D angle-interlock woven composites. Journal of Materials Chemistry and Physics. 2013;**140**:183-190

[34] Jin L, Niu Z, Jin B, Sun B, Gu B. Comparisons of static bending and fatigue damage between 3D angle-interlock and 3D orthogonal woven composites. Journal of Reinforced Plastics and Composites. 2012;**31**(14):935-945

[35] Ma Q, Wang K, Wang S, Liu H, Jin B, Jin L. Tensile damage mechanism of 3-D angle-interlock woven composites using acoustic emission events monitoring. Autex Research Journal. 2018;**18**(1):46-50

[36] Jin B, Li X, Mier R, Pun A, Joshi S, Nutt S. Parametric modeling, higher order FEA and experimental investigation of hat-stiffened composite panels. Journal of Composite Structures. 2015;**128**:207-220

[37] Jin B, Joshi S, Pun A, Nutt S. Design sensitivity of hat-stiffened composite panels. In: Proceedings of American Society for Composites Conference 2014; San Diego. 2014

[38] Wu H, Xu W, Shan D, Jin B. An extended GRN model for low stress triaxiality and application in spinning forming. Journal of Materials Processing Technology. 2019;**263**:112-128

[39] Jin B, Liu W, Patel H, Nutt S. Application of MSC NASTRAN UDS in modeling and analysis of a hybrid composite reinforced conductor core. In: Proceedings of MSC NASTRAN Conference 2013; Los Angeles. 2013

[40] Ma H, Xu W, Jin B, Shan D, Nutt S. Damage evaluation in tube spinnability test with ductile fracture criteria. International Journal of Mechanical Sciences. 2015;**100**:99-111